[13]H. Raether, in *Springer Tracts in Modern Physics, Ergebnisse der Exakten Naturwissenschaften*, edited by G. Höhler (Springer, Berlin, 1965), Vol. 38, p. 84.
[14]N. D. Lang and W. Kohn (report of work prior to publication).
[15]J. A. Appelbaum and D. R. Hamann, Phys. Rev. B **6**, 1122 (1972).
[16]S. C. Ying, J. R. Smith, and W. Kohn, J. Vac. Sci. Technol. **9**, 575 (1972).
[17]J. Bardeen, Phys. Rev. **49**, 653 (1936).
[18]D. E. Beck and V. Celli, Phys. Rev. B **2**, 2955 (1971); D. E. Beck, V. Celli, G. Lo Vecchio, and A. Magnaterra, Nuovo Cimento B **68**, 230 (1970).
[19]D. M. Newns, Phys. Rev. B **1**, 3304 (1970).
[20]D. M. Newns, J. Chem. Phys. **50**, 4572 (1969).
[21]A. U. Sidyakin, Zh. Eksp. Teor. Fiz. **58**, 573 (1970) [Sov. Phys.-JETP **31**, 308 (1970)].
[22]E. Gerlach, in *Molecular Processes on Solid Surfaces*, edited by E. Drauglis, R. D. Cretz, and R. I. Jaffee (McGraw-Hill, New York, 1969), p. 181.
[23]J. W. Gadzuk, J. Phys. Chem. Solids **30**, 2307 (1969).
[24]J. C. Inkson, Surf. Sci. **28**, 69 (1971).
[25]V. Peuckert, Z. Phys. **241**, 191 (1971).
[26]J. Rudnick, Phys. Rev. B **5**, 2863 (1972).
[27]J. Jackson, *Classical Electrodynamics* (Wiley, New York, 1962).
[28]P. R. Antoniewicz, J. Chem. Phys. **56**, 1711 (1972).
[29]E. A. Stern and R. A. Ferrell, Phys. Rev. **120**, 130 (1960).
[30]J. Heinrichs, Phys. Rev. B **7**, 3487 (1973).
[31]S. C. Ying, J. R. Smith, and W. Kohn, Phys. Rev. Lett. **30**, 610 (1973); quoted by N. D. Lang, in *Solid State Physics*, edited by H. Ehrenreich, F. Seitz, and D. Turnbull (Academic, New York, to be published).
[32]See, in particular, Fig. 15 in Lang's article, Ref. 31.
[33]C. Kittel, *Introduction to Solid State Physics* (Wiley, New York, 1956).
[34]The relative magnitude of the correction term in (3.50) is twice the correction found by Antoniewicz (Ref. 28). This is due to this author's use of a definition of the point-charge contribution (Ref. 19) which is twice as large as the corresponding true dipole moment defined by Eq.(3.4).
[35]R. H. Ritchie and A. L. Marusak, Surf. Sci. **4**, 234 (1966).
[36]D. Wagner, Z. Naturforsch. A **21**, 634 (1966).
[37]The explicit expression for $\delta n(z, k_\parallel, \omega)$ obtained in this way is somewhat different from the one given by Peuckert (Ref. 25) for the case of a fixed oscillating charge embedded in the surface. Indeed for a charge of the form (4.5) we find

$$\delta n(z, k_\parallel, \omega) = q \int_{-\infty}^{\infty} \frac{dk_z}{\epsilon(k, \omega)} \left([1-\epsilon(k, \omega)] \times \cos k_z (z - z_0) + \cos k_z (z + z_0) - \frac{2\cos k_z z}{1+\epsilon_s^{-1}(k_\parallel, \omega)} \int_{-\infty}^{\infty} \frac{dk'_z}{\pi} \frac{k_\parallel}{k_\parallel^2 + k_z'^2} \frac{\cos k'_z z_0}{\epsilon(k_\parallel, k'_z, \omega)} \right) \times \delta(\omega - \omega_0), \; z_0 > 0, \; z > 0,$$

instead of Peuckert's Eq. (39). In the present formulation, which is quite different from the one used by Peuckert, one would recover this author's expression by subtracting in the right-hand side of (4.19) both the fictituous surface charge density $\rho_s(k_\parallel, \omega)\delta(z)$ and the image of the embedded charge q. Such an expression, of course, does not define the true induced charge density.
[38]If one is interested in describing properly the long-wavelength behavior of $\epsilon(k, \omega)$ near the plasma frequency one must choose a different value for β. The value $\beta^2 = 3v_F^2/5$ which is usually adopted in this case reduces the dispersion relation for bulk plasmons to the RPA expression at long wavelengths.
[39]P. J. Feibelman, Surf. Sci. **27**, 438 (1971).
[40]*Handbook of Mathematical Functions*, edited by M. Abramowitz and I. A. Stegun (National Bureau of Standards, Washington, D.C., 1965), p. 228.
[41]N. Takimoto, Phys. Rev. **146**, 366 (1966).
[42]H. Boersch, J. Geiger, and W. Stickel, Z. Phys. **212**, 130 (1968).
[43]I. M. Franck, Usp. Fiz. Nauk **87**, 189 (1965) [Sov. Phys.-Usp. **8**, 729 (1966)].
[44]I. S. Gradshteyn and I. W. Ryzhik, *Tables of Integrals Series and Products* (Academic, New York, 1965).

PHYSICAL REVIEW B VOLUME 8, NUMBER 4 15 AUGUST 1973

Thermoelectric Effects in Pure and V-Doped Ti_2O_3 Single Crystals*

S. H. Shin,† G. V. Chandrashekhar, R. E. Loehman,‡ and J. M. Honig
Department of Chemistry, Purdue University, West Lafayette, Indiana 47907
(Received 12 February)

The Seebeck coefficient α for pure and V-doped Ti_2O_3 single crystals has been measured between 54 and 500 K. A very strong peak in α near 75 K for Ti_2O_3 is interpreted as arising from phonon-drag effects; this peak is missing for the V-doped specimens. Between 150 and 350 K the variation of α with temperature T could be interpreted in terms of a standard model for mixed conduction in a semiconductor. For $T > 350$ K, α diminished rapidly with increasing T, which reflects the semiconductor-semimetal transition that has been reported in the literature on the basis of conductivity studies. The effect of doping on thermoelectric phenomena has been investigated in detail and is found closely to parallel the effects encountered in conductivity measurements. An explanation is offered as to why V-doped Ti_2O_3 exhibits p-type characteristics. Values of relevant band parameters have been determined.

I. INTRODUCTION

There has been considerable interest in the electrical properties of Ti_2O_3; most of this work, which is largely confined to electrical conductivity studies, is summarized in several review articles.[1-4] Attention has been focused primarily on the electrical transition which occurs between approximately 400 and 600 K, in which range the material changes from a semiconductor to a semi-

metal. The origin of this transition was controversial for some time; however, it now seems generally agreed that this change arises from a gradual reduction of a band gap with an increase in temperature, which is followed by band overlap. These changes occur as a concomitant to a lattice distension without change of symmetry which coincides with the electrical transition.

In this connection it appeared of interest to investigate the thermoelectric properties of single crystals of pure and V-doped Ti_2O_3. The experiments were designed in part to follow up on one earlier study[5] and in part to carry through a set of thermoelectric measurements closely paralleling the resistivity investigations on V-doped Ti_2O_3 published elsewhere.[6] It will be demonstrated that the model proposed earlier for the transition[3,7,8] is consistent with the data cited below.

II. EXPERIMENTAL TECHNIQUE

Single crystals of Ti_2O_3 and V-doped Ti_2O_3 were grown by techniques detailed elsewhere.[8,9] Ancillary resistivity studies were carried out with a standard four-probe technique; provision was made for automatic recording of the voltage drop across the sample under steady current flow as a function of the specimen temperature. The direction of current flow was reversed periodically to permit the averaging out of spurious thermoelectric signals.

Thermoelectric measurements were carried out with a bridge technique pioneered by Testardi and McConnell.[10] Chromel-constantan thermocouples were used for the differential measurements and copper-constantan for averaged temperature measurements. The differential thermocouples and two copper wires for Seebeck-voltage measurements at low temperature were soldered into two holes 0.014-in. diameter with indium, using an ultrasonic vibrator. For measurements at higher temperatures gallium-copper-tin alloys[11] were employed as solder. Temperatures below 77 K were obtained by pumping on liquid nitrogen. After equilibrium was established at a given temperature, a heat pulse was sent through the sample by a momentary flow of current through a small heater attached to one side of the sample. This set up a small temperature gradient which first increased and then decreased with time; this signal and the concomitant thermoelectric voltage were fed into the two arms of an x-y recorder, thereby producing a straight line whose slope could be accurately determined and converted into Seebeck-coefficient readings. This procedure is at once faster, more convenient, and more accurate than the conventional point-by-point technique.

Due to sample size requirements it was impossible to cut single-crystal specimens of different orientations from the same boule. Consequently, effects later ascribed to crystal anisotropy might be partly masked by differences in sample stoichiometry and in purity of different boules used in these experiments. However, the orientation effects cited below agree with those reported in earlier investigations.[12]

III. EXPERIMENTAL RESULTS

The ancillary resistivity measurements for several crystal orientations of pure Ti_2O_3 are shown in Fig. 1. These results are consistent with the measurements of Yahia and Frederikse[5] but are slightly at variance with other studies,[6,7,13] where the slight hump, seen in Fig. 1, at temperatures just below the onset of the transition, is missing. The origin of this discrepancy is not immediately apparent. The activation energy computed from the straight-line portion of Fig. 1 is $\epsilon_a = 0.0318$ eV. A continuation of this plot into the low-temperature range is shown in the upper portion of Fig. 2; the remainder of the graph is discussed later.

The thermoelectric effects are shown in Figs. 3 and 4 as plots of the Seebeck coefficient versus temperature. The observations on pure Ti_2O_3 are again reasonably consistent with those of Ref. 5, although the maxima in the neighborhood of 75 K are much more pronounced, and the high-temperature behavior of the Seebeck coefficient differs

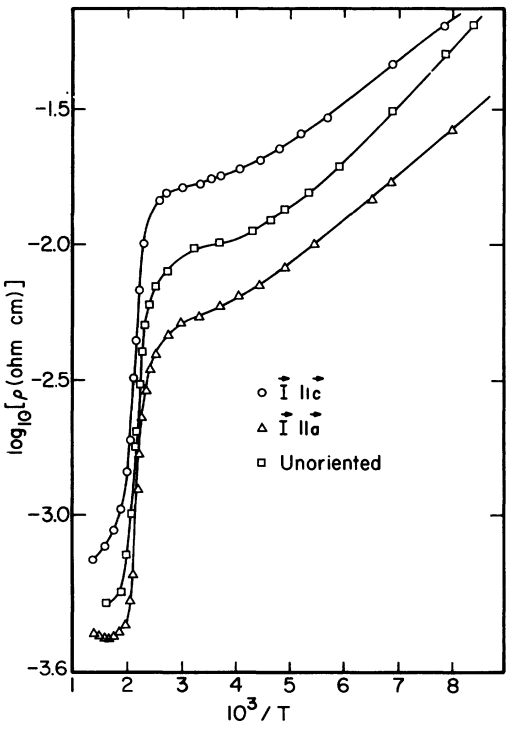

FIG. 1. $\log_{10} \rho$ vs $1/T$ for Ti_2O_3 in the transition-temperature range.

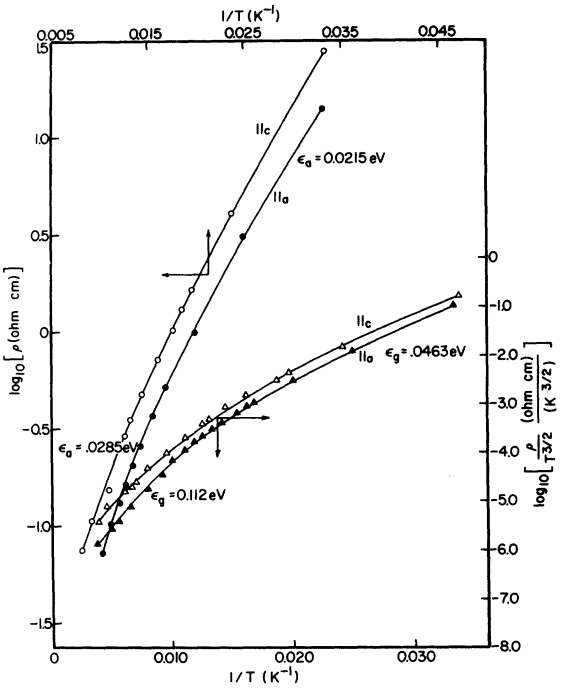

FIG. 2. $\log_{10}\rho$ and $\log_{10}\rho/T^{3/2}$ vs $1/T$ for Ti_2O_3 in the low-temperature range.

in some details from the earlier study.[5] As far as the present writers are aware, no prior work has been reported for thermoelectric effects in V-doped Ti_2O_3.

IV. DISCUSSION OF RESULTS

The results shown in Figs. 3 and 4 will be discussed under several headings: the high-temperature region, intermediate-temperature region, low-temperature region for pure Ti_2O_3, and the thermoelectric effects observed for doped Ti_2O_3. The high-temperature results above 400 K will be correlated with the semiconductor-metal transition in pure and doped Ti_2O_3. In the intermediate-temperature range between approximately 200 and 400 K the thermoelectric effects will be interpreted in terms of a conventional two-band model. The peak observed in the low-temperature range will be ascribed to phonon drag effects. Finally, a parallel will be drawn between the effects of doping on the thermoelectric properties and on the resistivity, as reported upon elsewhere.[6]

V. SEEBECK COEFFICIENT IN HIGH-TEMPERATURE RANGE

According to the currently accepted model, Ti_2O_3 is a nearly intrinsic semiconductor at low temperatures. This may be understood as follows: There is an incipient splitting of Ti $3d$ states into a number of sublevels under the influence of an incipient crystal field of the corundum lattice. A certain

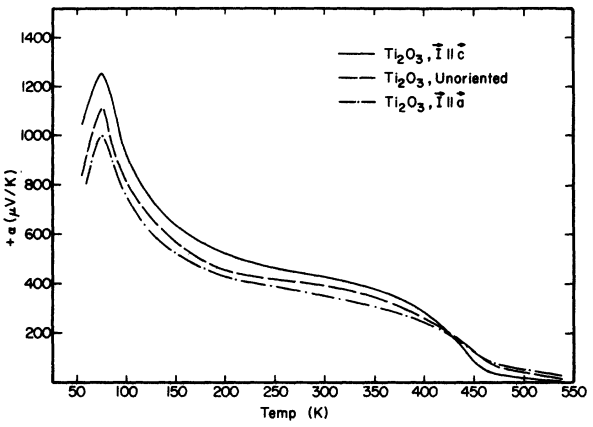

FIG. 3. Seebeck coefficients (α) vs T for Ti_2O_3.

degree of mixing of these states with O $2s$ and $2p$ states also occurs. This leads to a broadening of the levels into a series of relatively narrow bands of primarily d-type character. The lowest-lying band, of a_1 symmetry, is separated by a small gap (of the order of 0.1 eV, as shown below) from higher-lying bands of e symmetry. With rising temperature, the c parameter of the lattice is found to expand and the a parameter of the corundum lattice is found to contract over roughly the range between 400 and 600 K. As explained elsewhere,[7] this leads to a gradual diminution of band gap and ultimately produces the onset of overlap between the above-mentioned a_1 and e bands. Thus, one would anticipate a steady decrease in Seebeck coefficient α through the transition region, which is precisely what is observed. The details of the anticipated changes in α cannot be readily calculated because of two complications: First, the band gap and degree of band overlap are strong functions of temperature and are not accurately known; sec-

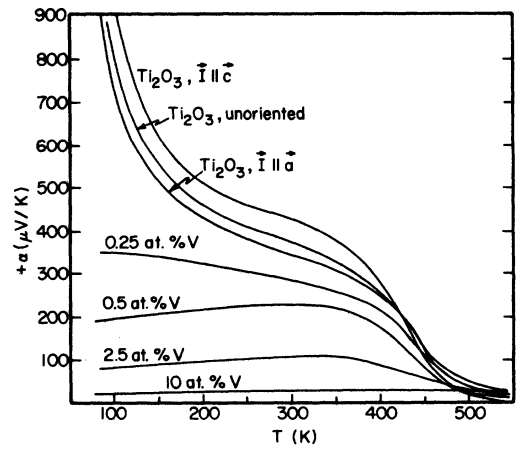

FIG. 4. Seebeck coefficients (α) vs T for $(Ti_{1-x}V_x)_2O_3$.

ond, there is a gradual changeover from classical statistics to degeneracy. The statistical theory of thermoelectric phenomena in the transition range is very complex; for this reason, no attempt was made to fit the observations between 380 and 550 K to a theoretical model.

That the above explanation is tenable is indicated by the fact that above 550 K all curves shown in Fig. 4 approach a common range. This is consistent with the concept that in the regime of overlapping bands the density of charge carriers is so high that the contributions arising from impurities or from vanadium doping exert only a secondary effect. It should be noted that the Seebeck coefficients are uniformly positive, indicating a preponderance of holes. This matter will be dealt with at greater length below.

VI. INTERMEDIATE-TEMPERATURE RANGE

Between 160 and 350 K the experimental findings are consistent with a standard two-band semiconductor model subject to classical statistics. This fact does not prove the model to be correct, but only that there is no need at present to invent a more complicated model for the interpretation of these data.

The specific assumptions on which the subsequent analysis is based are the following: (1) The material is a nearly intrinsic semiconductor such that $n_n,\ n_p \gg \frac{1}{2}(N_A - N_D)$ where n_n and n_p are the densities of charge carriers in the valence and conduction bands, respectively, and where N_A and N_D are the densities of acceptor and donor impurities, respectively. (2) It is assumed that formulas based on a band of standard form are appropriate, and that the use of classical statistics remains acceptable, i.e., that $-\mu_i/k_BT > 2$, where μ_i is the Fermi level calculated relative to the appropriate band edge. (3) The relaxation-time formalism is introduced in the theoretical analysis through the relation $\tau = \tau_0 \epsilon^{r-1/2}$, where τ is the relaxation time, τ_0 a quantity independent of the energy ϵ, and where r is the scattering index. (4) A number of parameters, introduced below, are assumed to be sensibly independent of temperature T. (5) The mobility is assumed to depend on temperature according to the relation $u_i(T) = u_i^0 T^{-l}$, where l is an adjustable parameter. In a number of cases, notably $SrTiO_3$[14] and $KTaO_3$,[15] l is empirically found to have values close to $l = 3$. We have verified that a temperature dependence in the range between T^{-2} and T^{-3} for the mobility simulates the theoretically anticipated temperature dependence $u \sim e^{(\hbar c k/k_B T)} - 1$, with $k \approx 250\ \mathrm{cm}^{-1}$. The exponential dependence is suggested by a theoretical analysis of the scattering of charge carriers by longitudinal optical phonons; a value $k \approx 250\ \mathrm{cm}^{-1}$ was selected as being consistent[16,17] with lattice vibration frequencies observed in Raman scattering experiments. Since the relevant k values are not accurately known, in the interest of simplicity we continue to use the approximate relation $u_i \sim T^{-3}$.

Preliminary calculations indicated that the strictly intrinsic model, characterized by the condition $n_n - n_p = 0$, did not fit the data nearly as well as the nearly intrinsic model described below. According to the standard theory,[18,19] the charge carrier density in each band is given by

$$n_n = -\tfrac{1}{2}(N_A - N_D) + [\tfrac{1}{4}(N_A - N_D)^2 + n^2]^{1/2},$$
$$n_p = +\tfrac{1}{2}(N_A - N_D) + [\tfrac{1}{4}(N_A - N_D)^2 + n^2]^{1/2}, \quad (1)$$

where

$$n^2 \equiv 4(2\pi m_n^{1/2} m_p^{1/2} k_B T/h^2)^3 e^{-\epsilon_G/k_B T}, \quad (2)$$

in which m_n and m_p are the effective masses of the carriers in their respective bands, and ϵ_G is the band-gap energy; all other symbols retain their conventional significance.

Since $n_n n_p = n^2$, the condition $n_n, n_p \gg \frac{1}{2}(N_A - N_D)$ cited earlier is equivalent to the requirement $n \gg \frac{1}{2}(N_A - N_D)$. Then Eq. (1) simplifies to

$$n_n = n - \tfrac{1}{2}(N_A - N_D), \quad n_p = n + \tfrac{1}{2}(N_A - N_D) \quad (3)$$

to first-order terms. The two-band conductivity now reads

$$\sigma = \sigma_n + \sigma_p = n_n e u_n + n_p e u_p$$
$$= ne(u_p + u_n) + \tfrac{1}{2}(N_A - N_D)e(u_p - u_n) \quad (4)$$

to terms of first order of smallness. According to Eq. (2), n varies exponentially with T, whereas u_i changes as $u_i \sim T^{-3}$; therefore, the temperature dependence of the total conductivity is dominated by the first term on the right-hand side of Eq. (4). This approximation should remain viable even if the condition $n \gg \frac{1}{2}(N_A - N_D)$ is not strictly satisfied, so long as one is only interested in the dependence of σ on T. Thus, in the first-order approximation the resistivity should be analyzed according to the relation

$$\rho = \rho_0 T^{l-3/2} e^{\epsilon_G/2k_B T} \quad (5)$$

in the temperature regime below the transition, where ϵ_G can be considered sensibly independent of T.

It was empirically found that plots of $\log_{10} \rho/T^{l-3/2}$ vs $1/T$ for $1/T > 3$ and with $l = 3$ or $3\frac{1}{2}$ yielded straight lines, in contradistinction to Fig. 1, which exhibits curvatures. The gaps calculated from these plots are entered in Table I; they are larger than those based on Fig. 1. This latter set will later be shown to be incompatible with the thermoelectric data.

A similar situation exists with respect to the Hall coefficient: From purely thermodynamic considera-

TABLE I. Tabulation of parameters useful in two-band analysis of transport properties for Ti_2O_3.

(a) Energy gaps, determined according to Eq. (5) from plots of $\log_{10}\rho/T^{l-3/2}$ vs $1/T$

l	ϵ_G (eV)
3	0.10_0
$3\frac{1}{2}$	0.11_8

(b) Charge carrier densities for Ti_2O_3 at 300 K, as determined from Eq. (8) with $R = 0.08$ cm^3/C $(1 < s < 2)$

σ_p/σ_n	n/s (10^{19} cm^{-3})
3	3.9
5	5.2
7	5.9

(c) Partial conductivities at 300 K, as determined from Eqs. (4) and (8)

	$\vec{l} \parallel \vec{a}$		$\vec{l} \parallel \vec{c}$	
σ_p/σ_n	σ_p (Ω cm)$^{-1}$	σ_n	σ_p (Ω cm)$^{-1}$	σ_n
3	13_9	48	46	16
5	15_6	30	51	10
7	16_3	23	54	7.8

(d) Parameters obtained from ϵ_G, Fig. 5, and Eq. (11)

	$\nabla T \parallel \vec{a}$				$\nabla \parallel \vec{c}$			
σ_p/σ_n	$\mu_n - \mu_p$ (eV)	μ_n (eV)	μ_p (eV)	A	$\mu_n - \mu_p$ (eV)	μ_n (eV)	μ_p (eV)	A
3	0.021	−0.039	−0.060	4.62	0.034	−0.034	−0.066	5.1
5	0.012	−0.044	−0.056	3.5	0.025	−0.038	−0.063	3.9
7	0.0072	−0.046	−0.054	3.1	0.021	−0.039	−0.061	3.5

(e) Upper limits on band gap (see text, Sec. VI)

σ_p/σ_n	$\nabla T \parallel \vec{a}$ ϵ_G (eV)	$\nabla T \parallel \vec{c}$ ϵ_G (eV)
3	0.18	0.23
5	0.135	0.18
7	0.12	0.16

tions it may be shown[20,21] that the two-band Hall coefficient is given by

$$R = s\,\frac{n_p e u_p^2 - n_n e u_n^2}{(n_p e u_p + n_n e u_n)^2}\ , \tag{6}$$

where s is the parameter occurring in the one-band Hall coefficients $R_i = Z_i\, s_i/n_i e$ $(Z_i = \pm 1)$. We shall assume here that $s_n = s_p \equiv s$; it may be shown that s_i ranges between $1 < 3\pi/8 \leq s_i \leq 315\pi/512 < 2$, depending on the value of the scattering index r. On introducing Eq. (1) into Eq. (6) and expanding, one obtains a very complicated relation whose zero-order term is given by

$$R = \frac{s}{ne}\left(\frac{u_p - u_n}{u_p + u_n}\right). \tag{7}$$

Another formulation, more relevant to our subsequent analysis, reads as follows:

$$R = \frac{s}{\sigma}\,\frac{\sigma_p u_p - \sigma_n u_n}{\sigma_p + \sigma_n} \approx \frac{s}{ne\sigma}\,(\sigma_p - \sigma_n) = \frac{s}{ne}\,\frac{\sigma_p/\sigma_n - 1}{\sigma_p/\sigma_n + 1}\ . \tag{8}$$

Finally, a standard thermodynamic analysis[20,21] based on irreversible thermodynamics shows that the two-band Seebeck coefficient is given by

$$\alpha = \frac{k_B}{e}\left[-\frac{\sigma_n}{\sigma}\left(A - \frac{\mu_n}{k_B T}\right) + \frac{\sigma_p}{\sigma}\left(A - \frac{\mu_p}{k_B T}\right)\right]\ , \tag{9}$$

where $A \equiv A_n = A_p$ is the transport parameter appearing in the expression for the one-band Seebeck coefficient $\alpha_i = (k_B/e)(A_i - \mu_i/k_B T)$, which, in the standard theory, has values in the range $2 \leq A_i \leq 4$, depending on the value of the scattering index r. As earlier, the quantity μ_i is given by $\mu_n \equiv \zeta - \epsilon_c$ and $\mu_p \equiv \epsilon_v - \zeta$, where ζ is the Fermi level relative to vacuum, and where ϵ_c and ϵ_v are the band edge energies for the conduction and valence bands, respectively. Since we are primarily concerned with temperature variations of quantities of interest it suffices to use the zero-order approximation, according to which $n_n \approx n_p \approx n$, where n is specified by Eq. (2). On introducing the relation $\epsilon_G = -\mu_n - \mu_p$ one obtains $n_n/n_p = (m_n/m_p)^{3/2} e^{(\mu_n - \mu_p)/k_B T}$. Using these relations it emerges that

$$\frac{\mu_n - \mu_p}{k_B T} = -\tfrac{3}{2}\ln\frac{m_n}{m_p} - \ln\frac{n_p}{n_n} = \frac{2\mu_n + \epsilon_G}{k_B T} \tag{10}$$

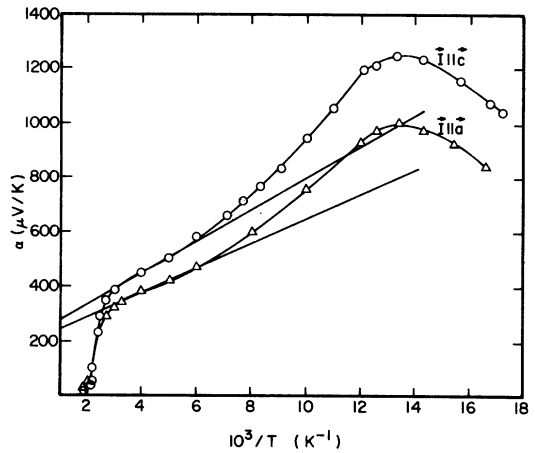

FIG. 5. Seebeck coefficients (α) vs $1/T$ for Ti_2O_3.

with which Eq. (9) may be reformulated as follows:

$$\alpha = \frac{k_B}{e}\left\{ A\,\frac{\sigma_p/\sigma_n - 1}{\sigma_p/\sigma_n + 1} + \left[\frac{\mu_n - \mu_p}{k_B} + \frac{\epsilon_G}{2k_B}\left(\frac{\sigma_p/\sigma_n - 1}{\sigma_p/\sigma_n + 1}\right)\right]\frac{1}{T}\right\}. \quad (11)$$

In applying the above to the data at hand, it should be recognized that we do not report here on any Hall-coefficient measurements. A search of the literature revealed that the value $R = 0.08$ cm^3/C represents a reasonable average for the Hall coefficient at room temperature. It is of interest that all R values reported in the literature are positive; according to Eq. (7) or (8) this means that $\sigma_p/\sigma_n > 1$. Furthermore, the intrinsic carrier density as computed from Eq. (8) is shown in Table I. For values of $\sigma_p/\sigma_n > 7$ the quantity n assumes rather large values, especially if the upper limit is used for s.

Equation (8) may be combined with the relation $\sigma = \sigma_p + \sigma_n$ to determine the one-band conductivities for pure Ti_2O_3 at room temperature. These results are also assembled in Table I.

The Seebeck-coefficient data were analyzed on the basis of Fig. 5 which shows the variation of α with $1/T$. According to Eq. (11) such a plot should be linear, whereas Fig. 5 shows that the straight-line region extends only over a very limited range. This fact may be attributed to several factors: First, the various parameters multiplying $1/T$ in Eq. (11) are not truly independent of temperature. Second, $\sigma = \sigma_p + \sigma_n$ changes very rapidly at temperatures above 400 K, thereby placing a lower limit on $1/T$ over which a straight-line relationship might be expected to apply. Third, the phonon drag effect becomes appreciable below 150 K, which places an upper bound on $1/T$ over which the straight-line relationship might be expected to apply. In these circumstances it makes sense to draw the straight-line section of Fig. 4 to be tangent to that portion of the curve which lies closest to the onset of the transition, so as to minimize the contributions associated with the phonon drag effect. Table I shows the values of the parameters needed to fit Eq. (11) to the slopes and intercepts of the straight lines shown in Fig. 5; in the above the relationship $\mu_n - \mu_p = 2\mu_n + \epsilon_G$ with $\epsilon_G = 0.11$ eV was utilized. Inspection of the table shows that for all three choices of σ_p/σ_n the Fermi level is found to be located rather close to the middle of the band gap, which is a very sensible result. The A parameters are also quite reasonable; as mentioned earlier these should lie in the range between 2 and 4. For $\sigma_p/\sigma_n < 3$, however, the A values get uncomfortably large.

It is noteworthy that the term $\epsilon_G(\sigma_p/\sigma_n - 1)/2k_B(\sigma_p/\sigma_n + 1)$ dominates $(\mu_n - \mu_p)/k_B$. Since the slope of the straight line in Fig. 5 is positive it is necessary to have $\sigma_p/\sigma_n > 1$, in agreement with deductions based on the Hall-coefficient determinations. If the term $(\mu_n - \mu_p)/k_B$ is neglected altogether, one can set an upper limit on the band gap as indicated by the listing shown in Table I. These limits are quite reasonable in light of available data. Finally, it should be observed that a gap of $\epsilon_G = 0.0636$ eV $= 2\epsilon_a$ based on Fig. 1 is incompatible with the data of Fig. 5 since negative values of the ratio σ_p/σ_n would then be required to match the slopes. The conclusion that $\sigma_p > \sigma_n$ very strongly implies that the bandwidth for the valence band is greater than that of the conduction band. Preliminary numerical calculations[22] are in reasonable agreement with the scheme proposed here.

VII. PHONON DRAG EFFECTS

A case will now be made for linking the marked peaks in Fig. 3 to the occurrence of phonon drag effects in Ti_2O_3. Aside from the fact that these peaks are similar to those reported where phonon drag effects are well documented, one may cite the following features in support of the above contention: (1) The peaks are absent in the $(V_xTi_{1-x})_2O_3$ alloys, presumably because impurity scattering now is the dominating mechanism for the various relaxation processes. (2) The size of this anomaly was greatly reduced in investigations involving impure samples. (3) No electrical anomalies of comparable magnitude have been observed in the resistivity measurements of Fig. 2 nor in preliminary Hall measurements over this temperature range. In both of these latter sets of measurements plots of $\log_{10}\rho$ and $\log_{10}R$ vs $1/T$ and plots of $\log_{10}\rho/T^{3/2}$ and $\log_{10}R/T^{3/2}$ vs $1/T$ showed only changes in slopes over the temperature range where the marked thermoelectric anomaly is encountered. (4) The data are reasonably consistent with the standard theories of phonon drag effects.

The theory, presented in great detail by Herring,[23,24] predicts that the excess Seebeck coefficient should vary with temperature as $\Delta\alpha \equiv \alpha - \alpha_d \propto T^{-7/2}$, where α is the observed Seebeck coefficient and α_d is the Seebeck coefficient ascribed to the normal diffusive type of thermoelectric effect. This expression is expected to apply on the high-temperature side of the peak and is predicted on the assumptions (a) that the dominant phonon-drag mechanism is through the interaction of electrons with acoustic phonons; (b) that the relationship $\omega = cq$ applies, where ω is the frequency, c is the velocity of sound, and q is the wave number of the phonon, the sound velocity being considered a constant; (c) that the collision processes are describable by a single mean free path or single relaxation time.

In the absence of a better procedure we elected to determine the quantity $\Delta\alpha$ by extending the straight-line portion of Fig. 5 as shown and computing the difference between the extrapolated portion and the observed value of α. It was found that plots of $\log_{10}\Delta\alpha$ vs $\log_{10}T$ were quite linear with the following slopes: -3.74 for $\vec{\nabla}T \parallel \vec{a}$, -4.43 for $\vec{\nabla}T \parallel \vec{c}$ in the low-temperature range, and -4.76 for $\vec{\nabla}T \parallel \vec{c}$ in the high-temperature range. These values are somewhat larger than the value of -3.5 anticipated from the theoretical analysis. However, it should be kept in mind that the slopes are quite sensitive to the extrapolation procedures and that the theoretical analysis leading to this result is highly approximate. The main point to be made is that $\Delta\alpha$ is a very strong function of T, as is expected for the phonon drag effect.

While the peak values shown in Fig. 3 are relatively large compared to α values outside the peak range, they are quite small compared to peak values of over 17 000 μV/K reported for pure Ge near 20 K, and of 32 500 μV/K cited for ZnO (at 77 K, α was still rising strongly with diminishing temperature in this case).[24] The comparatively small peak values of $\Delta\alpha$ which we observed may be attributed to several factors. First, Ti_2O_3 as grown is not stoichiometric and is frequently highly compensated. As mentioned earlier, impurities diminish the size of the peak. Second, according to the present band model, both electrons and holes contribute to conduction phenomena in Ti_2O_3. Accordingly, in a thermoelectric experiment carriers of both signs are dragged towards the cold end of the specimen. This leads to a partial cancellation of effects and renders the observed value smaller than it would have been had carriers of only one type participated in conduction processes.

Unfortunately, lack of appropriate experimental facilities precluded measurements of α below 55 K; hence, there was no opportunity to check whether data taken at temperatures below the peak followed the $T^{1/2}$ law which is presumed to hold for phonon drag effects on the low-temperature side of the peak.

VIII. EFFECTS OF DOPING ON THERMOELECTRIC PROPERTIES

The effect of V doping on the thermoelectric properties of Ti_2O_3 is shown in Fig. 4. As is obvious, the addition of V_2O_3 markedly reduces the Seebeck-coefficient values in the temperature range 77–400 K, relative to those encountered in the pure host material. It has been shown in earlier work[6] that addition of V_2O_3 introduces holes into the valence band of the host lattice roughly in proportion to the density of the dopant. One thereby soon reaches a state in which the density of charge carriers in the valence band greatly exceeds that of the conduction band, so that the two-band model used earlier becomes inapplicable. For sufficiently high doping concentrations the mixed material is expected to become metallic—a fact which is borne out by the small values of α observed for doping levels in excess of 2 at.%.

Preliminary thermoelectric measurements were carried out by Eklund[25] in the range from 4 to 82 K. The Seebeck coefficient of a specimen containing nominally 4-at.% V remained constant at $\alpha = +115$ μV/K between 80 and 38 K and then diminished steadily towards $\alpha = 0$ with decreasing temperature. There was no evidence for the existence of a phonon-drag peak for this sample in the temperature range under investigation.

There is a very good parallelism between the observations reported here and the experiments pertaining to the effects of doping on the resistivity of the material. Chandrashekhar *et al.*[6] report that the incremental addition of V_2O_3 to Ti_2O_3 diminishes the size of the semiconductor-semimetal transition, but does not change the temperature range over which this transition occurs; moreover, for doping in excess of 4 at.% the material remains metallic. Correspondingly, one observes in Fig. 4 a progressive decrease in the variation of α with T in the transition temperature region with increasing doping, while the temperature range in which this transition occurs remains basically unaffected. Just as in the resistivity measurements, the initial addition of V_2O_3 to Ti_2O_3 has a much larger effect than any subsequent additions. Above a doping level of 4 at.% α varies very little with T and, in some instances, increases with T, as might be expected for a *bona fide* metal. Finally, if one adopts the very elementary model according to which the Fermi level and charge carrier density in a metal are related by $\mu_p = (h^2/2m)(3n/8\pi)^{2/3}$, and in which the Seebeck coefficient is specified by $\alpha = +\pi^2 k_B^2 T/3e\mu_p$, then it is predicted that α should vary with doping concentration as $n^{-2/3}$ at constant temperature, on the assumption that the charge carrier concentra-

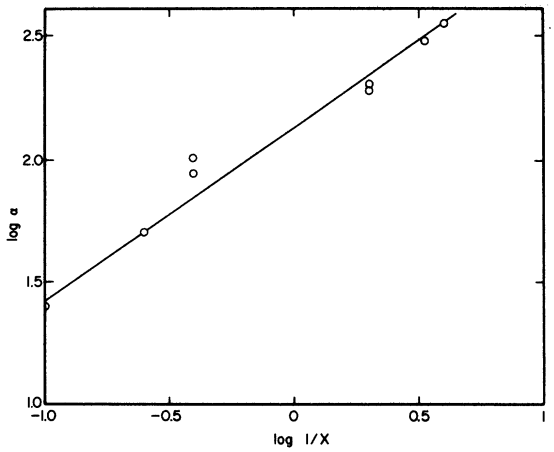

FIG. 6. $\log_{10}\alpha$ vs $\log_{10}1/x$ for $(Ti_{1-x}V_x)_2O_3$.

tion is dominated by the impurity concentration in the specimen. Figure 6 shows that a plot of $\log_{10}\alpha$ vs $\log_{10}1/x$, obtained by reading off appropriate values at 100 and 300 K from Fig. 6 does give rise to a reasonably straight line with a slope of 0.71. This is in good agreement with the above elementary predictions, and disagrees rather more seriously with the value of $\frac{4}{9}$ derived by Van Cong and Mesnard[26] for a heavily doped semiconductor.

IX. SUMMARY AND FURTHER DISCUSSION

The principal findings arising out of this research are the following: (a) An analysis of the conductivity, Hall-, and Seebeck-coefficient measurements shows that the band gap in Ti_2O_3 near room temperature is in the range 0.10–0.12 eV. This represents an upward revision from values cited elsewhere.[3,7,8,12] The mobility of charge carriers varies with temperature roughly as T^{-3}. (b) Seebeck- and Hall-coefficient measurements show that the partial conductivity of holes exceeds that of electrons by factors in the range from 3 to 7; the ratio of widths of the valence and conduction bands also falls in this range. This represents a revision of the mirror-image band scheme utilized by Honig and Reed[8] in their analysis of magnetoresistance effects. As indicated in that reference, this simplification was introduced at the time solely to minimize the number of disposable parameters. Also, the qualitative band-structure diagrams[4,7] presented in the literature need be revised in the manner indicated by the above conclusion. (c) The very marked peak in the Seebeck coefficients of pure Ti_2O_3 single crystals near 75 K is ascribed to a phonon drag mechanism. (d) The effect of doping Ti_2O_3 with V on the Seebeck coefficient is quite analogous to the effect described elsewhere[6] on the resistivity; the basic conclusions drawn in that publication concerning the mechanism of the transition are thus reinforced by the present study.

The above data also conform to a number of earlier magnetic susceptibility measurements[27–29] which show an increase in paramagnetic susceptibility with rising temperature. This phenomenon was attributed[29] to the generation of charge carriers as a concomitant to the increasing band overlap in the region of the electrical transition.

Finally, it should be noted that the present work offers one possibility for rationalizing the rather puzzling observation that V-doped Ti_2O_3 is p type, despite the fact that V contains one more d electron than does Ti. The explanation hinges on the fact that V doping is known to narrow the band-gap.[30,31] Hence at fixed temperature, a vanadium-doped sample contains more carriers than a pure specimen. Since the hole mobility greatly exceeds the electron mobility or the mobility of charge carriers in the V impurity band, the effect of doping with V is to retain the p-type characteristics of the undoped specimens.

*Supported by the ARPA-IDL and NSF-MRL Program at Purdue University.

†Present address: Department of Physics, Yeshiva University, New York, N. Y.

‡Present address: Department of Metallurgical and Materials Engineering, University of Florida, Gainesville, Fla. 32601.

[1]D. Adler, Rev. Mod. Phys. **40**, 714 (1968).

[2]D. Adler, in *Solid State Physics*, edited by F. Seitz, D. Turnbull, and H. Ehrenreich, (Academic, New York, 1968) Vol. 21, p. 1.

[3]J. M. Honig, Rev. Mod. Phys. **40**, 748 (1968).

[4]J. B. Goodenough, in *Progress in Solid State Chemistry*, edited by H. Reiss (Pergamon, Oxford, England, 1971), Vol. 5, p. 145.

[5]J. Yahia and H. P. R. Frederikse, Phys. Rev. **123**, 1257 (1961).

[6]G. V. Chandrashekhar, Q. Won Choi, J. Moyo, and J. M. Honig, Mater. Res. Bull. **5**, 999 (1970).

[7]L. L. Van Zandt, J. M. Honig, and J. Goodenough, J. Appl. Phys. **39**, 594 (1968).

[8]J. M. Honig and T. B. Reed, Phys. Rev. **174**, 1020 (1968).

[9]T. B. Reed, R. E. Fahey, and J. M. Honig, Mater. Res. Bull. **2**, 561 (1967).

[10]R. L. Testardi and G. K. McConnell, Rev. Sci. Instrum. **32**, 1067 (1961).

[11]G. G. Harman, Rev. Sci. Instrum. **31**, 717 (1960).

[12]J. M. Honig, L. L. Van Zandt, T. B. Reed, and J. Sohn, Phys. Rev. **182**, 863 (1969).

[13]S. C. Abrahams, Phys. Rev. **130**, 2230 (1963).

[14]H. P. R. Frederikse, W. R. Thurber, and W. R. Hosler, Phys. Rev. **134**, A442 (1964).

[15]S. H. Wemple, M. Di Domenico, Jr., and A. Jayaraman, Phys. Rev. **180**, 547 (1969).

[16]A. Mooradian and P. M. Raccah, Phys. Rev. B **3**, 4253 (1971).

[17]S. H. Shin, R. Aggarwal, B. Lax, and J. M. Honig (unpublished research).

[18]J. S. Blakemore, *Solid State Physics* (Saunders, Philadelphia, Pa. 1969).

[19]T. P. McKelvey, *Solid State and Semiconductor Physics* (Harper and Row, New York, 1966).

[20]T. C. Harman and J. M. Honig, *Thermoelectric and Thermomagnetic Effects and Applications* (McGraw-Hill, New York, 1967).

[21]A. H. Wilson, *Theory of Metals*, 2nd ed. (Cambridge U. P., Cambridge, England, 1953).
[22]I. Nebenzahl and M. Weger, Philos. Mag. **24**, 1119 (1971).
[23]C. Herring, Phys. Rev. **96**, 1163 (1954).
[24]C. Herring, *Semiconductors and Phosphors*, edited by M. Schön and H. Welker (Vieweg, Braunschweig, Germany, 1958), p. 184.
[25]P. Eklund (private communication).
[26]H. Van Cong and G. Mesnard, Phys. Status Solidi B **50**, 53 (1972).
[27]A. D. Pearson, J. Chem. Phys. **5**, 316 (1958).
[28]L. K. Keys and L. N. Mulay, Phys. Rev. **154**, 453 (1967).
[29]G. J. Hyland, Phys. Status Solidi **35**, K133 (1969).
[30]T. Kawakubo, T. Yanagi, and S. Nomura, J. Phys. Soc. Jap. **15**, 2102 (1960).
[31]R. E. Loehman, C. N. R. Rao, and J. M. Honig, J. Phys. Chem. **73**, 1781 (1969).

PHYSICAL REVIEW B VOLUME 8, NUMBER 4 15 AUGUST 1973

Anharmonic Lattice Dynamics in K

M. S. Duesbery and Roger Taylor
Division of Physics, National Research Council, Ottawa, Ontario, Canada

H. R. Glyde
Atomic Energy of Canada Limited, Chalk River Nuclear Laboratories, Chalk River, Ontario, Canada

(Received 13 December 1972)

The lattice dynamics of K at $T = 9$, 99, 215, and 299 °K is studied employing an effective pair ion-ion potential and the self-consistent (SC) theory for anharmonic crystals. The effective potential was derived from first principles following the method that Geldart *et al.* developed successfully for Na. The purpose of the present paper is (i) to test whether the potential derivation can be extended successfully to K and (ii) to compare the SC anharmonic theory with experiment and the standard anharmonic perturbation theory used by Buyers and Cowley. For all the symmetry directions except the Δ_1 branch, the phonon frequencies computed here at 9 °K lie within 2% of the observed frequencies verifying the validity of the K ion-ion potential. The total anharmonic shifts in frequency (quasiharmonic + anharmonic) with temperature are comparable but $\sim$ 20% greater than those computed by Buyers and Cowley. Given the scatter in the observed shifts, both calculations agree equally well with experiment.

I. INTRODUCTION

In a recent paper Glyde and Taylor[1] presented calculations of phonon frequencies and lifetimes in Na over the temperature range $T = 5$–361 °K using the self-consistent theory of anharmonic lattice dynamics. To describe Na an effective ion-ion potential, derived from the calculations of Geldart *et al.*,[2] which employs the Geldart-Taylor[3] screening function, was used. The encouraging agreement between theory and experiment both at liquid-nitrogen and room temperatures in Na has prompted us to do a similar calculation for K, where there are data available,[4,5] to test extensions of this method.

As in the case of Na there can be found in the literature (e.g., see the review article by Joshi and Rajagopal[6]) large numbers of lattice dynamic calculations for K using a wide variety of models in the harmonic approximation. However, to our knowledge only Buyers and Cowley[5] have calculated anharmonic contributions to the phonon frequencies and lifetimes of K. In their calculations, Buyers and Cowley employed a semiempirical pseudopotential with parameters chosen by fitting the computer harmonic phonon dispersion curves to those observed at 9 °K. This potential was then used to compute the quasiharmonic and the cubic and quartic anharmonic contributions to the phonon frequencies and lifetimes at higher temperatures via standard perturbation theory. Their calculated frequency shifts and lifetimes gave reasonable agreement with their experimental results at 99, 215, and 299 °K.

As in the case of Na the present interatomic potential is derived following the procedure of Geldart *et al.*[2] and Basinski *et al.*[7] This is more fundamental in the sense that no fitting to solid data is employed. The derivation is discussed briefly in Sec. II. The resulting phonon frequencies calculated using the self-consistent theory are then presented and discussed in Sec. III.

II. THEORETICAL MODEL

A. Effective Ion-Ion Potential

To compute the effective ion-ion potential, a knowledge of both the bare electron-ion interaction and the conduction-electron dielectric function is necessary. In K, where nonlocal effects are not important, the interionic potential may be written in the form